Point defects in the flux-line lattice of superconductors

Enrick Olive, Ernst Helmut Brandt

Point defects in the flux-line lattice of superconductors

Enrick Olive and Ernst Helmut Brandt
Max Planck Institut für Metallforschung, P.O. Box 800665, D-70506 Stuttgart, Germany
(Received 24 November 1997)

The self-energy and interaction energy of vacancies and interstitials in the triangular lattice of parallel Abrikosov vortices in type-II superconductors are calculated within London theory. Various stable and metastable equilibrium configurations of the flux-line lattice around such point defects are investigated. The vacancy with highest (sixfold) symmetry usually does not exhibit the lowest energy, as was already found by Frey *et al.* [Phys. Rev. B **49**, 9723 (1994)]. Due to the relaxation of the surrounding vortex lattice, the defect energies are very small compared with the binding energy of one vortex. The interaction of point defects is weak and can be repulsive or attractive, depending on their type and distance and on the ratio of the magnetic penetration depth λ to the average vortex spacing a. In the limit $\lambda \gg a$ these results should be applicable to thin films in a perpendicular magnetic field. [S0163-1829(98)04521-4]

I. INTRODUCTION

After the prediction of the flux-line lattice (FLL) in the type-II superconductors by Abrikosov,[1] decoration experiments by Träuble and Essmann[2] succeeded in observing the FLL at the specimen surface with high resolution. This Bitter decoration revealed a more or less defective lattice, containing vacancies, interstitials, dislocations, partial dislocations, stacking faults, and even disclinations.[3] The properties of edge and screw dislocations in the FLL were discussed first in Refs. 4. The energy of flux-line vacancies with sixfold symmetry was calculated both at low inductions (from London theory, Ref. 5) and high inductions (from the linearized Ginzburg-Landau theory, Ref. 6). In a detailed paper considering also the thermal proliferation of point defects in a FLL ''supersolid,'' Frey *et al.*[7] found that during relaxation of the surrounding FLL the vacancy with sixfold symmetry in the FLL is unstable with respect to a compression along one of the three axes connecting the nearest neighbors of the vacancy, but the energy of the final configuration is very close to this saddle-point configuration with sixfold symmetry. Our computations below confirm this finding. The role of defects and plastic deformation during thermally activated motion of the lattices of vortex lines and of vortex disks (''pancakes''[8]) in conventional superconductors and in layered high-T_c superconductors was discussed by several authors, see, e.g., Refs. 9,10 and the review papers, Refs. 11–15.

As shown recently,[16,17] the self-energies and interaction energies of unrelaxed point defects in soft lattices are compensated almost completely by the relaxation energy of the surrounding lattice. In *isotropic* lattices this compensation is even perfect, and the resulting defect energies thus vanish, if one applies the continuum approximation and linear elasticity theory and disregards the shear modulus. In soft lattices (with smooth long-range interaction) the continuum approximation is very good, and the shear modulus is much smaller than all other moduli. In *anisotropic* lattices a finite defect energy results even in these approximations, e.g., in the three-dimensional (3D) lattice of pancake vortices[16,17] in layered superconductors. If the lattice sums defining such defect energies are evaluated exactly, the self-energies and interaction energies of point defects are finite but very small, being differences of two large terms.

In the present paper we compute the configuration and energy of an infinite periodic arrangement of various point defects in the lattice of parallel Abrikosov flux lines. The periodicity originates from the periodic boundary conditions which we imply to avoid surface effects originating in finite systems. The interaction energy of defects is then obtained from the dependence of the defect energy on the periodicity lengths L_x and L_y, and in the limit of large periodicity lengths the self-energy of the defects results, since the interaction goes to zero.

The outline of this paper is as follows. In Sec. II we describe our computational method and define the defect energies. The results are presented in Sec. III, and Sec. IV summarizes our main findings.

II. COMPUTATIONAL METHOD

A. Interaction potential

We consider the static (zero-temperature) energy of arbitrary arrangements of parallel vortex lines (along z) in the London limit, which applies when the Ginzburg-Landau (GL) parameter $\kappa=\lambda/\xi \gg 1$ is large and the distances r_{ij} between the vortex lines are much larger than the radius of the vortex cores $r_c \approx \xi$. Here λ is the magnetic penetration depth and ξ the superconducting coherence length. Practically, the London limit means that the induction B is much less than the upper critical field $B_{c2}=\Phi_0/(2\pi\xi^2)$ and that the (repulsive) interaction between the flux lines is purely magnetic,

$$V(r_{ij}) = E_0 K_0(r_{ij}/\lambda). \tag{1}$$

Here $E_0=\Phi_0^2/(2\pi\mu_0\lambda^2)$ is an energy per unit length (in the following we shall put $E_0=1$), $K_0(x)$ is a modified Bessel function with the limits $K_0(x)\approx\ln(1/x)$ $(x\ll 1)$, and $K_0(x)$ $\approx(\pi/2x)^{1/2}\exp(-x)$ $(x\gg 1)$. If κ is not large, the interaction between vortices is not only a magnetic repulsion but there is also an attractive contribution of range $\xi/\sqrt{2}$, originating from the gain in superconducting condensation energy when

the vortex cores overlap. Thus, the effective interaction is approximately $V(r)\propto K_0(r/\lambda)-K_0(\sqrt{2}r/\xi)$, which has a finite value at $r=0$.[18] In the special case $\kappa=1/\sqrt{2}$ both contributions compensate such that $V(r)\equiv 0$, which is an exact result in this special case, i.e., all vortex configurations have the same energy if $\kappa=1/\sqrt{2}$.

In Fourier representation the potential (1) reads

$$V(r)=\int \frac{d^2k}{4\pi^2}\tilde{V}(k)e^{i\mathbf{k}\cdot\mathbf{r}}, \tag{2}$$

$$\tilde{V}(k)=E_0\frac{2\pi}{k^2+\lambda^{-2}}. \tag{3a}$$

To facilitate the numerical evaluation of sums over reciprocal lattice vectors below, we multipy $\tilde{V}(k)$, Eq. (3a), by a convergence factor $\exp(-ck^2)$ with $c\to 0$. This heuristic cutoff converges more rapidly than the difference of two Lorentzians which would follow from the effective potential $V(r)\propto K_0(r/\lambda)-K_0(\sqrt{2}r/\xi)$; see Ref. 19 for the discussion of various vortex-core cutoffs. The Gaussian cutoff factor is equivalent to a convolution of $V(r)$ with the Gaussian $(1/\pi r_0^2)\exp(-r^2/r_0^2)$ of half width $r_0=2\sqrt{c}$, which removes the logarithmic infinity of $V(r)$ at $r=0$ and slightly enhances $V(r)$ at larger distances, since the volume $\int V(r)d^2r$ remains constant. To lowest order in r_0^2, the enhancement is obtained by the Taylor expansion of $V(|\mathbf{r}-\mathbf{r}'|)$ around $\mathbf{r}$, yielding $V(r)\to V(r)+(r_0^2/4)\nabla^2V(r)+O(r_0^4)$. For the London potential (1), this convolution gives the enhancement $K_0(r/\lambda)\to K_0(r/\lambda)(1+r_0^2/4\lambda^2)$. Thus, up to small terms of order $O(r_0^4)$ the potential (1) may be replaced by a modified potential with Fourier transform

$$\tilde{V}(k)=E_0\frac{2\pi}{k^2+\lambda^{-2}}\frac{\exp(-r_0^2k^2/4)}{1+r_0^2/4\lambda^2}. \tag{3b}$$

The inner cutoff r_0 plays the role of a vortex core radius. It is thus related to the coherence length $\xi\approx r_0$ (Refs. 19,20) and to the Ginzburg-Landau parameter by $\kappa=\lambda/\xi\approx\lambda/r_0$. Since we are mainly interested in the extreme London limit $\kappa\to\infty$, we shall choose $r_0\ll a$, e.g., $r_0=a/20$, where $a=(2\Phi_0/\sqrt{3}B)^{1/2}$ is the average spacing of the vortices in the ideal triangular lattice. The choice $r_0/a=1/20$ guarantees that always $B/B_{c2}=(4\pi/\sqrt{3})(\xi/a)^2\ll 1$ in our simulation. Thus, the only parameter which matters here is λ/a, related to B and to the lower critical field $B_{c1}\approx\Phi_0\ln\kappa/(\sqrt{8}\pi\lambda^2)$ by $B/B_{c1}\approx(\lambda/a)^2(4\pi\sqrt{2/3})/\ln\kappa\approx(10/\ln\kappa)(\lambda/a)^2$.

B. Periodic boundary conditions

The interaction energy of an arbitrary arrangement of vortices with positions $\mathbf{r}_i$ extended periodically with periodicity lenghts L_x and L_y to the infinite xy plane is in each (e.g., rectangular) periodicity cell of area $A=L_xL_y$ containing N vortices (vortex density $N/A=B/\Phi_0$),

$$U_N=\frac{1}{2}\sum_{i=1}^{N}{\sum_{j=1}^{\infty}}'\;V(r_{ij})=\frac{1}{2}\sum_{i=1}^{N}{\sum_{j=1}^{N}}'\;V_e(\mathbf{r}_{ij})+\frac{N}{2}U_{\rm per}, \tag{4}$$

with $\mathbf{r}_{ij}=\mathbf{r}_i-\mathbf{r}_j$. The dash at the j sum excludes the term $j=i$. $V_e(\mathbf{r})$ is an effective interaction potential between two vortices inside one periodicity cell including the interaction with the ''image lines'' positioned at $\mathbf{r}_i+\mathbf{R}$ where $\mathbf{R}=\mathbf{R}_{mn}=(mL_x+nL_y)$ $(m,n$ integer) are the vectors of the ''superlattice.'' This effective interaction is periodic and may thus be expressed as a Fourier series,

$$V_e(\mathbf{r})=\sum_{\mathbf{R}}V(\mathbf{r}+\mathbf{R})=\int\frac{d^2k}{4\pi^2}\tilde{V}(k)e^{i\mathbf{k}\cdot\mathbf{r}}\sum_{\mathbf{R}}e^{i\mathbf{k}\cdot\mathbf{R}}$$

$$=\frac{1}{A}\sum_{\mathbf{K}}\tilde{V}(K)\cos\mathbf{K}\cdot\mathbf{r}=\frac{2\pi}{A}\sum_{\mathbf{K}}\frac{\cos\mathbf{K}\cdot\mathbf{r}}{K^2+\lambda^{-2}}. \tag{5}$$

Here $\mathbf{K}=\mathbf{K}_{\mu\nu}$ are the reciprocal lattice vectors of the superlattice, e.g., $\mathbf{K}_{\mu\nu}=2\pi(\mu/L_x,\nu/L_y)$ for the rectangular basic cell of area $A=L_xL_y$. In Eq. (5) we have used a general formula for 2D lattices with cell area A,

$$\sum_{\mathbf{R}}e^{i\mathbf{k}\cdot\mathbf{R}}=\frac{4\pi^2}{A}\sum_{\mathbf{K}}\delta_2(\mathbf{k}-\mathbf{K}), \tag{6}$$

where $\delta_2(x,y)$ is the 2D delta function and the infinite sums run over all real ($\mathbf{R}$) and reciprocal ($\mathbf{K}$) lattice vectors.

The constant $NU_{\rm per}/2$ in Eq. (4) originates from the interaction of each vortex with its own ''images,'' which had dropped out from the first sum in Eq. (4) when the terms $j=i$ were omitted. This term does *not* depend on the vortex positions, such as the vortex self-energies, which are also omitted in the interaction energy (4). However, since $NU_{\rm per}$ depends on the periodicity lengths L_x and L_y, this term is important when the energies of periodicity cells of various shape or size are compared. In particular, when $U_{\rm per}$ is disregarded, then the interaction-energy per vortex U_N/N of the infinitely large ideal FLL *artificially* depends on the choice of the periodicity area, see Table II in Ref. 7. Explicitly one has

$$U_{\rm per}=\sum_{\mathbf{R}\neq 0}V(R)=\int\frac{d^2k}{4\pi^2}\tilde{V}(k)\left(\sum_{\mathbf{K}}e^{i\mathbf{K}\cdot\mathbf{r}}-1\right)=\frac{1}{A}\sum_{\mathbf{K}}\tilde{V}(K)$$

$$-\int\frac{d^2k}{4\pi^2}\tilde{V}(k)\approx\frac{2\pi}{A}\sum_{K\le K_1}\frac{1}{K^2+\lambda^{-2}}-\frac{1}{2}\ln(1+K_1^2\lambda^2). \tag{7}$$

The cutoff radius K_1 in the last line of Eq. (7) should be chosen so large that the sum contains many terms, say $10^4\cdots 10^5$. The logarithm in this line results from integration of $\tilde{V}(k)$, Eq. (3a), over the circular area $k\le K_1$. The approximation (7) means that for $K\ge K_1$ the sum is replaced by an integral; the two integrals over the outer region $k\ge K_1$ then cancel.

Equation (4) is easily checked by considering the interaction energy of one vortex with all other vortices in an infinite ideally periodic lattice. This energy is twice the binding energy $U_B=U_N/N$ of a vortex; it is the same for all vortices; and it does not depend on the choice of the supercell. The factors 1/2 in Eq. (4) appear since in the infinite sums all pair interactions were counted twice. Finally, the term $U_{\rm per}/2$ is

the same for ideal and defective lattices since it does not depend on the vortex positions $\mathbf{r}_i$ but only on the size and shape of the periodicity cell.

The energy of ideal periodic vortex lattices may be easily computed by a single sum over the interactions $\propto K_0(R/\lambda)$. If λ is very large one may transform this infinite sum over ideal lattice points $\mathbf{R}$ into an expression of the form (7), where now the $\mathbf{R}$ and $\mathbf{K}$ are interpreted as the vectors and reciprocal vectors of the vortex lattice. The precision of this computation is considerably enhanced if the sum is not cut off abruptly at $K=K_1$ but smoothly, e.g., by multiplying the terms of the sum by a factor $\frac{1}{2}+\frac{1}{2}\tanh[1.9(K_1-K)/K_{\min}]$ (the factor 1.9 was found to optimize the accuracy), e.g., choosing $K_1=400K_{\min}$ and summing over $K\leqslant 410K_{\min}$ with $K_{\min}$ the shortest K. In this way we get for the binding energy of the triangular FLL with $K_{mn}^2=(16\pi^2/3a^2)(m^2+mn+n^2)$ (m,n integer)

$$U_B(a/\lambda)=\frac{U_N^{\rm ideal}}{N}=\frac{1}{2}\sum_{\mathbf{R}\neq 0}K_0(R/\lambda)=\frac{2\pi}{\sqrt{3}}\frac{\lambda^2}{a^2}-\frac{1}{2}\ln\frac{\lambda}{a}-\alpha(\lambda/a), \tag{8}$$

where the constant α is found numerically as $\alpha=0.754486$ for $\lambda/a\to\infty$ and $\alpha=0.884512$, 0.792504, 0.764426, 0.757000, 0.754890, 0.754587, 0.754512, 0.754490, 0.754487, 0.754486 for $\lambda/a=0.25$, 0.5, 1, 2, 5, 10, 20, 50, 100, 1000. Using $E_0=\Phi_0^2/(2\pi\mu_0\lambda^2)$ and $B=2\Phi_0/\sqrt{3}a^2$, one finds from Eq. (8) in the limit $\lambda\gg a$ the energy density of the ideal FLL $(B/\Phi_0)E_0U_B=B^2/2\mu_0$ as it should be.

C. Definition of defect energies

The energy of a superlattice of defects which do not change the number N of vortices in the periodicity area, naturally is defined as the difference between the energies of the defective and the ideal vortex lattices per periodicity cell,

$$U_d=U_N^{\rm defect}-U_N^{\rm ideal}. \tag{9}$$

Examples for such defects are one vacancy and one interstitial per supercell (of area $A=L_xL_y$) or a pair of edge dislocations.

Defects which change the number of vortices in the supercell, e.g., one vacancy or one interstitial, should be considered at constant vortex density $N/A=B/\Phi_0$. This definition has the additional advantage that the self-energy of the vortex lines drops out, $U_{\rm self}\approx\frac{1}{2}E_0\ln\kappa$ (for $\kappa\gg 1$). For example, generating a vacancy means that one removes one vortex and rebuilds it into the ideal vortex lattice; this is easily possible for large systems with many vacancies. For a finite supercell, the concrete procedure to add the removed vortex again without generating a new defect, is less obvious. But if $N\gg 1$ is not too small, one may replace this process by a subsequent linear elastic uniform compression which restores the original average vortex spacing a.[17]

The energy of a superlattice of vacancies in our infinite vortex lattice is conveniently computed as follows. The energy per vacancy, or per supercell with $N-1$ vortices and area A, is defined by

$$U_{\rm vac}=U_{N-1}^{\rm vac}-U_{N-1}^{\rm ideal}=U_{N-1}^{\rm vac}-\frac{N-2}{N}U_N^{\rm ideal}+U_{\rm corr}^{\rm vac}. \tag{10}$$

The second line in Eq. (10) was written such that $U_{\rm corr}^{\rm vac}$ is a small correction of the order of $U_B/N=U_N^{\rm ideal}/N^2$. The second line in Eq. (10) allows us to compute the ideal-lattice energy $U_N^{\rm ideal}$ by the same numerical method used also for the energy of the defective lattice (since the index is N, not $N-1$). This means near compensation (in a small difference of large terms) of the inaccuracies which may originate from the approximate potential (3b) and its numerical calculation or interpolation.

As stated above, the ideal binding energy U_B, Eq. (8), depends only on the ratio a_N/λ where $a_N=(2A/\sqrt{3}N)^{1/2}\propto N^{-1/2}$ is the ideal vortex spacing at constant supercell area $A=L_xL_y$. Thus one may write

$$U_{\rm corr}^{\rm vac}=\frac{N-2}{N}U_N^{\rm ideal}-U_{N-1}^{\rm ideal}=(N-2)U_B(a_N)-(N-1)U_B(a_{N-1}). \tag{11}$$

Since $U_{\rm corr}^{\rm vac}$ is small, it may be calculated from the exact binding energy $U_B(a/\lambda)$ as described above Eq. (8), even though the remaining terms in $U_{\rm vac}$, Eq. (10), are computed using the approximate potential (3b). This consideration is important since the vacancy energy after relaxation is expected to be very small, requiring high precision (or identical approximations) in the calculation of the large terms in the difference, Eq. (10). In the limit $\lambda\gg a$, one has from Eq. (8) $U_B=(2\pi/\sqrt{3})(\lambda/a)^2$. Inserting this into Eq. (11) one obtains

$$U_{\rm corr}^{\rm vac}\approx\frac{2\pi}{\sqrt{3}}\frac{\lambda^2}{a_N^2}\left[N-2-\frac{(N-1)^2}{N}\right]\approx -U_B/N=-U_N^{\rm ideal}/N^2. \tag{12}$$

Similarly, one finds for a superlattice of interstitials the energy per supercell,

$$U_{\rm int}=U_{N+1}^{\rm int}-U_{N+1}^{\rm ideal}=U_{N+1}^{\rm int}-\frac{N+2}{N}U_N^{\rm ideal}+U_{\rm corr}^{\rm int}, \tag{13}$$

with the small correction

$$U_{\rm corr}^{\rm int}=\frac{N+2}{N}U_N^{\rm ideal}-U_{N+1}^{\rm ideal}=(N+2)U_B(a_N)-(N+1)U_B(a_{N+1}). \tag{14}$$

In the limit $\lambda\gg a$ this gives

$$U_{\rm corr}^{\rm int}\approx\frac{2\pi}{\sqrt{3}}\frac{\lambda^2}{a_N^2}\left[N+2-\frac{(N+1)^2}{N}\right]\approx -U_B/N=-U_N^{\rm ideal}/N^2\approx U_{\rm corr}^{\rm vac}. \tag{15}$$

Thus, for $\lambda\gg a$ the two small corrections $U_{\rm corr}^{\rm vac}$ and $U_{\rm corr}^{\rm int}$ are equal. Note that in the definitions and results (10)–(15) it was not assumed that N is large. These formulas apply, therefore, to arbitrary order in $1/N$.

TABLE I. Energies of point defects at constant line density B/Φ_0 for several sizes of the periodicity cell $(L_x, L_y) = (5, 6\sqrt{3}/2)ta$ with $t = 1, 2, 3, 4, 5$. Listed are the self-energies of vacanices ($U_{\rm vac}$) and interstitials ($U_{\rm int}$) for various symmetries, see text, for three ranges of the vortex interaction $\lambda/a = 100$, 1, and 0.25. The energy unit is $E_0 = \Phi_0^2/(2\pi\mu_0\lambda^2)$.

$\lambda/a = 100$

t	$U_{\rm vac}^{\rm V6}$	$U_{\rm vac}^{\rm V3}$	$U_{\rm vac}^{\rm V2}$	$U_{\rm int}^{\rm EI}$	$U_{\rm int}^{\rm CI}$
1		0.10484	0.10235	0.07152	0.07174
2	0.12382	0.10768	0.10507	0.07354	0.07265
3	0.12411	0.10801	0.10571	0.07387	0.07286
4	0.12421	0.10811	0.10594	0.07398	0.07296
5	0.12425	0.10815	0.10606	0.07403	0.07300

$\lambda/a = 1$

t	$U_{\rm vac}^{\rm V6}$	$U_{\rm vac}^{\rm V3}$	$U_{\rm vac}^{\rm V2}$	$U_{\rm int}^{\rm EI}$	$U_{\rm int}^{\rm CI}$
1		0.09422	0.09230	0.06533	0.06536
2	0.11148	0.09701	0.09489	0.06703	0.06603
3	0.11179	0.09735	0.09548	0.06730	0.06620
4	0.11190	0.09746	0.09569	0.06739	0.06628
5	0.11195	0.09751	0.09578	0.06743	0.06632

$\lambda/a = 0.25$

t	$U_{\rm vac}^{\rm V6}$	$U_{\rm vac}^{\rm V3}$	$U_{\rm vac}^{\rm V2}$	$U_{\rm vac}^{\rm V2'}$	$U_{\rm int}^{\rm EI}$	$U_{\rm int}^{\rm CI}$
1		0.02433	0.02450	0.02454	0.02072	0.02034
2	0.02767	0.02560	0.02557	0.02555	0.02079	0.02009
3	0.02788	0.02580	0.02578	0.02573	0.02078	0.02006
4	0.02796	0.02587	0.02584	0.02579	0.02078	0.02005
5	0.02801	0.02591	0.02587	0.02581	0.02078	0.02005

When $N \gg \lambda^2/a^2$ is large, consideration of the term $\frac{1}{2}\ln(\lambda/a)$ in U_B, Eq. (8), contributes to $U_{\rm corr}$, a constant (N independent) term that dominates when $a^2 \ll \lambda^2 \ll L_x^2 \approx a^2 N$. In this limit one finds from Eqs. (11) and (14)

$$U_{\rm corr}^{\rm vac,\,int} \approx \pm\frac{1}{2}\left(\ln\frac{\lambda}{a} - \frac{1}{2}\right). \tag{16}$$

In this case these two correction terms have different signs for vacancy (>0) and interstitial (<0), but they are still much smaller in magnitude than the binding energy $U_B \approx 3.6(\lambda/a)^2 \gg 1$. For our computations below we shall compute the correction term from the exact Eqs. (11) and (14), using for U_B the algorithm described above Eq. (8) when $\lambda/a \gg 1$, or from the sum over modified Bessel functions in Eq. (8) when $\lambda/a \approx 1$. Inclusion of this correction term allows the precise computation of defect energies, which depend on the size and shape of the supercell.

Generalizing the expressions (10)–(16) to defects with n vortices added to the supercell (e.g., $n = -2$, -1, 1, 2, respectively, for double vacancy, vacancy, interstitial, and double interstitial) we find the energy per defect

$$U_{\rm def} = U_{N+n}^{\rm def} - U_{N+n}^{\rm ideal} = U_{N+n}^{\rm def} - \frac{N+2n}{N}U_N^{\rm ideal} + U_{\rm corr}^{\rm def}, \tag{17}$$

with the small correction

$$U_{\rm corr}^{\rm def} = \frac{N+2n}{N}U_N^{\rm ideal} - U_{N+n}^{\rm ideal}$$
$$= (N+2n)U_B(a_N) - (N+n)U_B(a_{N+n}) \tag{18}$$
$$\approx \frac{2\pi}{\sqrt{3}}\frac{\lambda^2}{a_N^2}\frac{n^2}{N} - \frac{n}{2}\left(\ln\frac{\lambda}{a} - \frac{1}{2}\right) \quad (\lambda \gg a). \tag{19}$$

One can show that this defect energy vanishes as it should be, when the defect disappears, i.e., when during relaxation the vortices rearrange to an ideal lattice again. The correction (18) also vanishes in the trivial case $n = 0$, i.e., when the defect consists of an equal number of vacancies and interstitials, see Sec. III D.

III. RESULTS

A. Computations

The lattice relaxation was performed by a quasistatic method using the effective interaction potential $V_e(x,y)$, Eq. (5), with Fourier transform (3b),

$$V_e(\mathbf{r}) = \frac{2\pi}{L_x L_y}\sum_{\mathbf{K}}\frac{\cos\mathbf{K}\cdot\mathbf{r}}{K^2+\lambda^{-2}}\,\frac{\exp(-r_0^2K^2/4)}{1+r_0^2/4\lambda^2} \tag{20}$$

in energy units $E_0 = \Phi_0^2/(2\pi\mu_0\lambda^2)$ and with $r_0 = a/20$, $a = (2\Phi_0/\sqrt{3}B)^{1/2}$. To accelerate the computation we tabulate $V_e(x,y)$ and its three derivatives V_x, V_y, and $V_{xy} = V_{yx}$ on a

TABLE II. Energy of vacancy-interstitial pairs U_{pair} at constant line density. The periodicity cell sizes are $(L_x, L_y) = (5, 6\sqrt{3}/2)ta$ with $t = 1, 2, 3, 4, 5$. The symmetry of each point defect in the pair is also listed.

	$\lambda/a = 100$	
t	U_{pair}	Defect symmetries
1	0.12555	V2 and CI′
2	0.17468	V2 and CI′
3	0.17802	V2 and CI′
4	0.17880	V2 and CI′
5	0.17910	V2 and CI
	$\lambda/a = 0.25$	
t	U_{pair}	Defect symmetries
1	0.03432	V2 and CI′
2	0.04517	V2 and CI′
3	0.04581	V2 and CI′
4	0.04591	V2′ and CI
5	0.04592	V2′ and CI

dense two-dimensional grid, from which we interpolate $V_e(x,y)$ rapidly using the bicubic routine of Ref. 21.

We used two different routines to minimize the total energy U_N, Eq. (4). The first routine is the standard conjugate-gradient method described in detail in Ref. 21. In our second minimization method the components x_i and y_i of the vortex positions are changed by a displacement proportional to the ratio of the first and second partial derivatives of the energy U_N with respect to this component, e.g.,

$$x_i := x_i - p\,\frac{\partial U_N/\partial x_i}{\partial^2 U_N/\partial x_i^2}. \tag{21}$$

The proportionality coefficient p in Eq. (21) is chosen as $p < 1$, and sometimes $p \ll 1$, which guarantees good convergence and stability of the method (''under-relaxation''). This relaxation method is symmetric since the $2N$ coordinates of the N vortices are all changed simultaneously within the same step after the $2N$ first and $2N$ second partial derivatives have been calculated. This second method approximately describes the relaxation of vortices which experience a viscous drag force proportional to their velocity. Since the curvatures $\partial^2 U_N/\partial x_i^2 \approx \partial^2 U_N/\partial y_i^2$ are roughly constant for all vortices $(i = 1 \ldots N)$, the effective viscosity is approximately constant and proportional to $1/p$.

Whereas the conjugate-gradient method may trap the system in one of the metastable states, the second method successively visits several metastable states. Any metastable state found by this second method and then inserted as an input configuration into the conjugate-gradient method, was then observed to be ''stable.'' We shall compare our results with those obtained by Frey *et al.*,[7] which were computed by methods adapted from molecular-dynamics simulations and using an Ewald sum technique.

To calculate the interaction between periodically arranged point defects we consider periodicity cells of various sizes. The number of independent positions of flux lines is $N = 30t^2$, contained within a rectangular basic cell of size $(L_x, L_y) = (5, 6\sqrt{3}/2)ta$, where $t = 1, \ldots, 5$ is an integer and a the lattice spacing. These numbers were chosen such that the rectangular box approximates a square to within 4%. Similar almost quadratic periodicity cells also where chosen in Refs. 7,22.

We present here numerical calculations for three different ratios of the magnetic penetration depth λ to the ideal vortex spacing a, namely, $\lambda/a = 100$, 1, and 0.25. As discussed below Eq. (3b), $\xi/a \approx r_0/a = 1/20$ was held constant in our computations, thus $B/B_{c2} \approx (4\pi/\sqrt{3})/20^2 \approx 0.02$, and our λ/a values mean $\kappa \approx \lambda/\xi \approx 2000$, 20, and 5; thus one always has $\kappa \gg 1$ and $B \ll B_{c2}$, which means the London theory is applicable. Since $B/B_{c1} \approx (10/\ln\kappa)(\lambda/a)^2$, our values λ/a correspond to reduced inductions $B/B_{c1} \approx 1.3 \times 10^4$, 3.4, and 0.4. From our results below one sees that the case $\lambda/a = 100$ is the extreme London limit $\kappa \gg 1$ with strongly overlapping vortex fields, and even the case $\lambda/a = 1$ differs little from this limit. Our results for $\lambda/a \geq 1$ should thus be compared to those of Ref. 7, which considers the limit $\lambda \to \infty$. In our third example, $\lambda/a = 0.25$, the vortices interact only with a few nearest neighbors.

B. Vacancies

To create a superlattice of vacancies we start from the ideal triangular lattice and remove one flux line per supercell. After relaxation we then find four different equilibrium configurations exhibiting sixfold, fourfold, threefold, and twofold axial symmetry around the vacancy (V6, V4, V3, V2), see Fig. 1 for examples. One can see that the center of symmetry of all these configurations is the initial vacancy position. The fourfold symmetry will not be considered further in the following since it is supposed to be an artifact due to our rectangular periodicity cell. The sixfold symmetry configuration for the smallest box size $(L_x, L_y) = (5, 6\sqrt{3}/2)a$, i.e., for $t = 1$, also will not be considered further since it was not found to be a metastable state for this small box size. The other vacancy types were metastable in the sense that our ''viscous'' relaxation method remained stationary at these configurations during many iteration steps before it continued to find a configuration with lower energy.

The vacancy energy was computed from Eqs. (10) and (11). Our results are displayed in Fig. 2 and Table I. We find that for all three λ/a ratios the lower the symmetry is, the lower is the final vacancy energy. Our periodic boundary conditions mean that we have a rectangular superlattice of defects. Since we change only the size of the periodicity cell and not its shape, i.e., $L_x/L_y = 0.96$, the total energy of such a superlattice of defects should exhibit qualitatively the same distance dependence as the interaction between two single defects in a large periodicity cell. In particular, if the interaction between two point defects at a distance r follows a power law $U \approx r^{-\alpha}$, the energy of a superlattice of such defects will follow the same power law and our method gives the correct exponent α.

For each type of vacancy we find that the defect energy increases with increasing size $L_x \times L_y$ of the periodicity cell. From this we conclude that *the interaction between two vacancies is attractive* whatever their symmetry is. This conclusion is in contradiction with the findings of a repulsive interaction between twofold symmetric vacancies in Ref. 7.

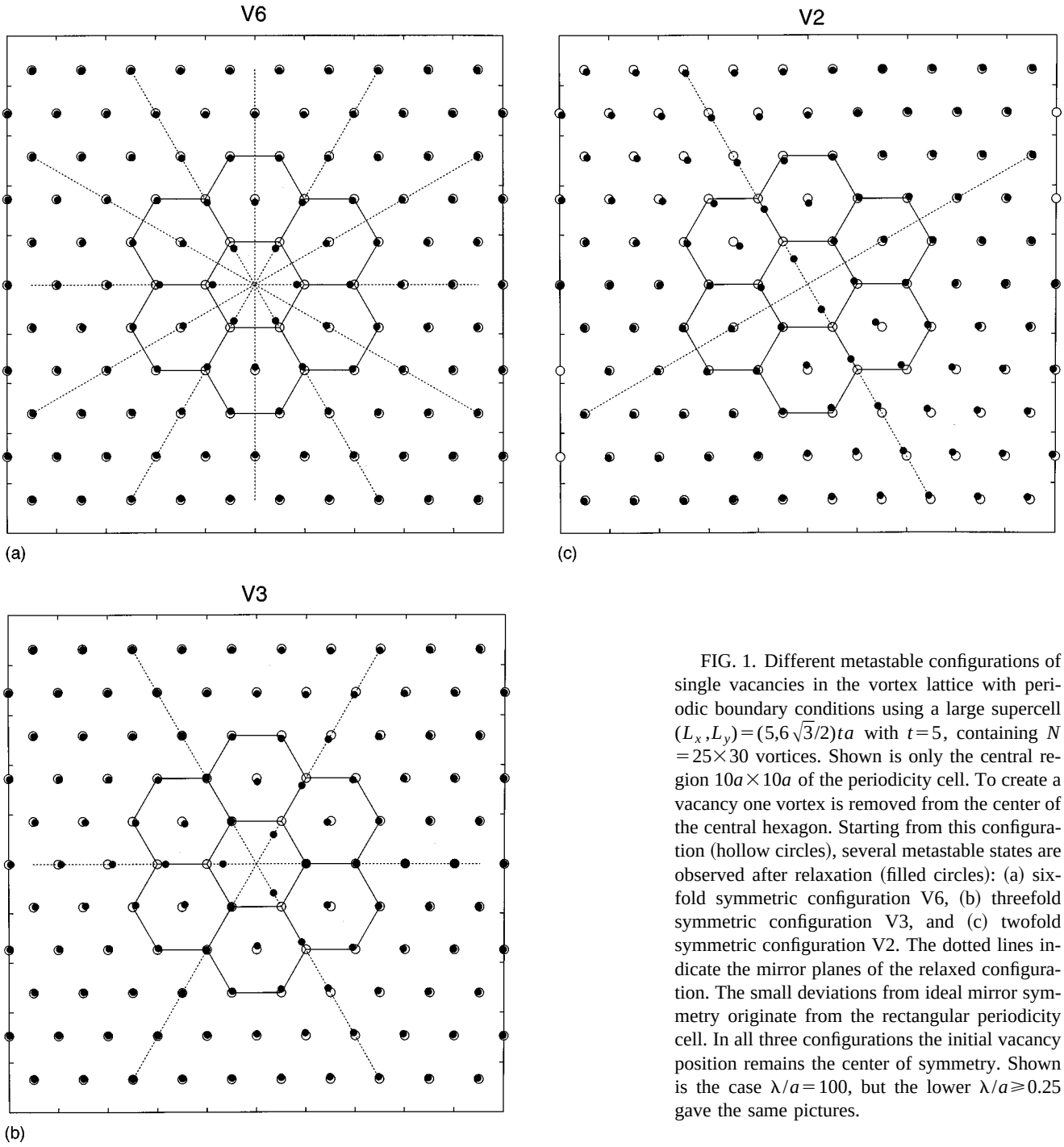

FIG. 1. Different metastable configurations of single vacancies in the vortex lattice with periodic boundary conditions using a large supercell $(L_x, L_y) = (5, 6\sqrt{3}/2)ta$ with $t = 5$, containing $N = 25 \times 30$ vortices. Shown is only the central region $10a \times 10a$ of the periodicity cell. To create a vacancy one vortex is removed from the center of the central hexagon. Starting from this configuration (hollow circles), several metastable states are observed after relaxation (filled circles): (a) sixfold symmetric configuration V6, (b) threefold symmetric configuration V3, and (c) twofold symmetric configuration V2. The dotted lines indicate the mirror planes of the relaxed configuration. The small deviations from ideal mirror symmetry originate from the rectangular periodicity cell. In all three configurations the initial vacancy position remains the center of symmetry. Shown is the case $\lambda/a = 100$, but the lower $\lambda/a \geq 0.25$ gave the same pictures.

With the lowest value of λ/a, a qualitatively new result appears, see Fig. 2(c). Now we find that the lower energy does no longer correspond to the vacancy V2 which has a twofold symmetry axis through the initial vacancy position, but to a new configuration V2′ with a twofold symmetry axis through a vortex position as shown in Fig. 3. Starting with this new configuration V2′, we have observed its metastability also for $\lambda \geq 1$. In these cases, the energy of this configuration is very close to the energy of the vacancy V2 but slightly higher.

C. Interstitials

Starting from the ideal triangular lattice, we added one flux line per supercell to create a superlattice of interstitials. Two different types of interstitials were investigated: the centered interstitial (CI) positioned in the center of a triangle formed by three neighboring flux lines, and the edge interstitial (EI) which sits in the middle between two flux lines.

After relaxation both types of interstitials keep their original symmetry, see Fig. 4 for examples of such configurations. This means that the CI remains in the center of a triangle and hence has threefold symmetry. In the case of the EI, the relaxation of the surrounding flux lines proceeds mainly in one of the nearest-neighbor directions of the ideal triangular lattice. Thus the original twofold symmetry is preserved. The interstitial energies are computed from Eqs. (13) and (14). In Fig. 5 we plot the energies for both types of interstitials versus the linear size L_x of the basic box, see also

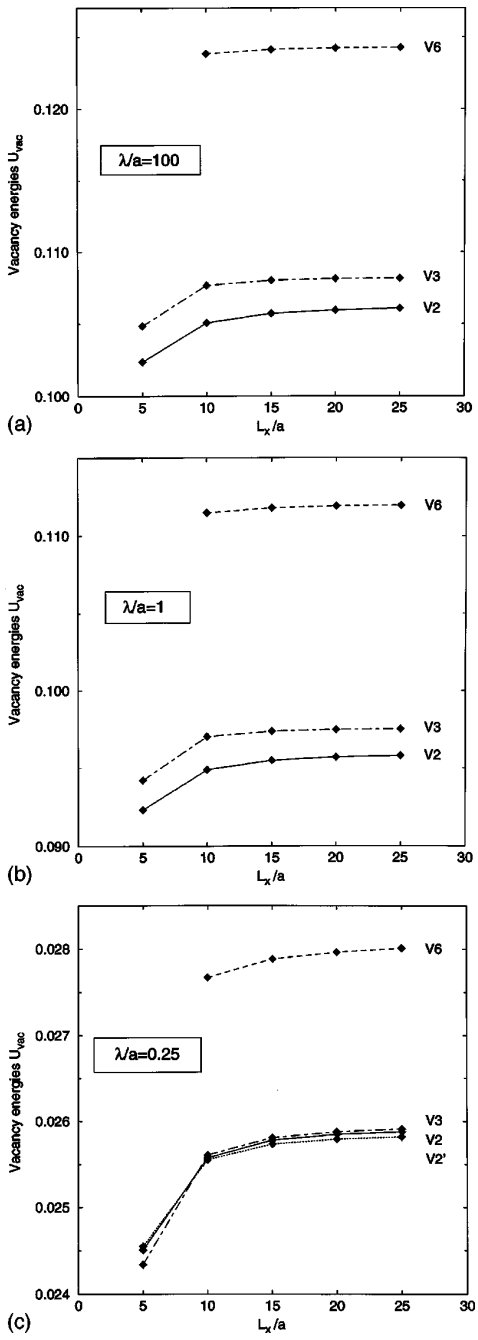

FIG. 2. Supercell-size (or distance) dependence of the defect energies for the sixfold symmetric vacancy V6 (dashed line), threefold symmetric vacancy V3 (dash-dotted line), and twofold symmetric vacancy V2 (solid line). The energy in units of E_0 is plotted versus L_x/a where L_x and $L_y=1.04L_x$ are the sides of the rectangular periodicity box and a is the lattice spacing. Results are presented for (a) $\lambda/a=100$, (b) $\lambda/a=1$, and (c) $\lambda/a=0.25$. The lower the symmetry is, the lower is the vacancy energy. In the case $\lambda/a=0.25$ a new configuration V2′ is reached (see Fig. 3) which has lower energy (dotted line) than V2. For all three λ/a values the interaction between vacancies (whatever their symmetry) is attractive for distances $L_x>5a$.

Table I. One can see that the CI always has a lower energy than the EI. Thus, in contrast to the vacancies, the higher the symmetry of the interstitial is, the lower is the final defect energy.

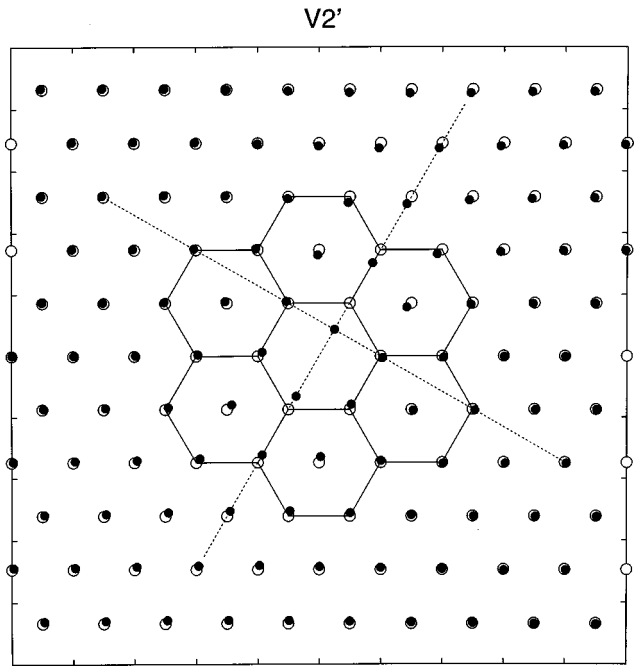

FIG. 3. The new vacancy configuration V2′ obtained for the box size $(L_x,L_y)=(5,6\sqrt{3}/2)ta$ with $t=5$, presented as in Fig. 1. In the case $\lambda/a=0.25$ this new vacancy type has a lower energy than the vacancy V2 shown in Fig. 1(c). One can see that the two mirror planes (dotted lines) cross at a flux line and not at the initial vacancy position. Thus, the initial vacancy position is no longer the center of symmetry.

The energies of the CI and EI interstitials increase with increasing size of the basic box for $\lambda/a\geqslant 1$. This implies *attractive interactions* for both EI and CI at distances larger than five lattice spacings a. But for $\lambda/a=0.25$ the situation is different. In this case, the CI shows a *repulsive interaction* at distances $L_x>5a$. For the EI, we observe a *repulsive interaction* for distances $L_x>10a$. But for smaller distances the energy decreases with decreasing size of the periodicity cell, which means an *attractive interaction* of such interstitials at distances between five and ten lattice spacings.

Finally, one can notice that the self energies of the interstitial are lower than those of the vacancies. Hence, as already found by Frey *et al.*,[7] the interstitials, rather than the vacancies, are energetically favored, and among them the centered interstitial has the lower energy.

D. Vacancy-interstitial pairs

As a third case, we considered vortex configurations with one vacancy and one interstitial per periodicity cell, choosing $\lambda/a=100$ and $\lambda/a=0.25$ as above. In Secs. III B and III C we have shown that the lower energy configurations for an isolated vacancy correspond to a twofold symmetry (either V2 for $\lambda/a=100$ and $\lambda/a=1$ or V2′ for $\lambda/a=0.25$), and for an isolated interstitial to a threefold symmetry (centered interstitial CI for all values of λ/a). In the present subsection we investigate the interaction between these point defects and describe how the twofold and threefold local symmetries of the vacancies and interstitials change when the distance between them becomes finite.

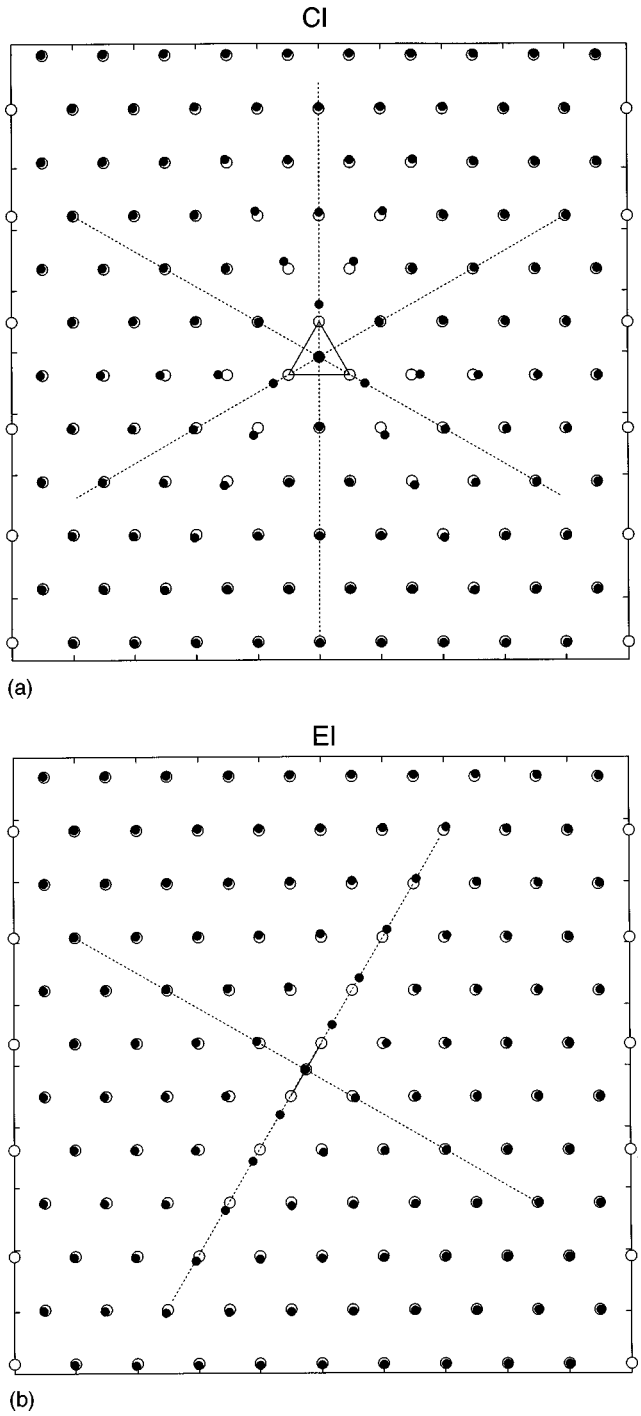

FIG. 4. The interstitial configurations obtained for the rectangular box size $(L_x, L_y) = (5, 6\sqrt{3}/2)ta$ with $t = 5$, presented as in Fig. 1. To create a superlattice of interstitials in the triangular vortex lattice, one flux line per supercell is inserted either (a) in the center of a triangle to create a centered interstitial CI, or (b) in the middle between two flux lines to create an edge interstitial EI. Starting from these situations (hollow circles), the relaxed configurations (filled circles) keep their original symmetry. The dotted lines show the mirror planes of these configurations. In both cases, the interstitial is the center of symmetry.

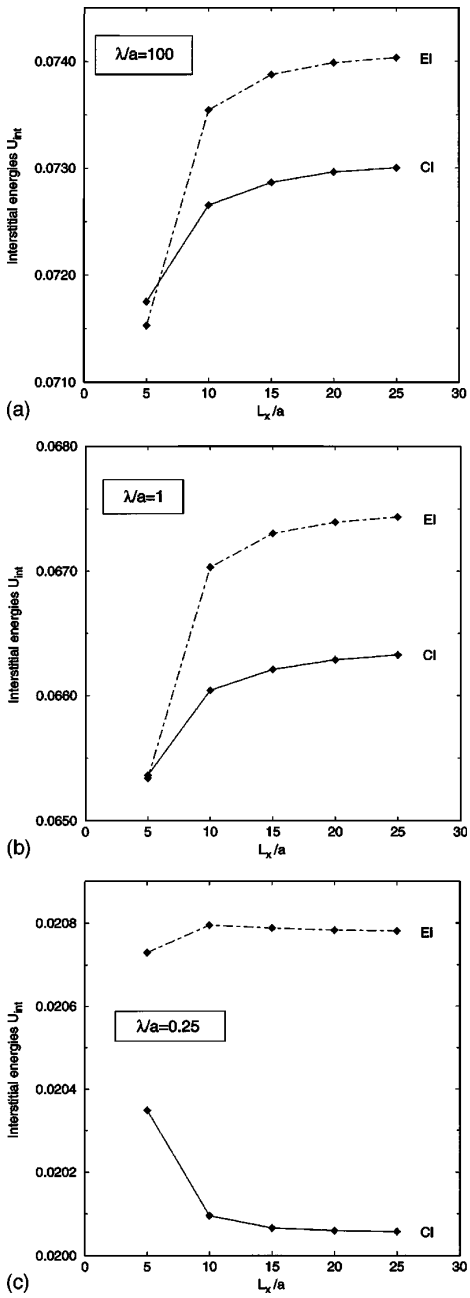

FIG. 5. Supercell size dependence of the defect energies for the centered interstitial (solid line) and for the edge interstitial (dash-dotted line). The energy in units of E_0 is plotted versus L_x/a where L_x is one side of the (almost quadratic) periodicity box and a is the lattice spacing. Results are presented for (a) $\lambda/a = 100$, (b) $\lambda/a = 1$, and (c) $\lambda/a = 0.25$. For all three λ/a values the centered interstitial has a lower energy than the edge interstitial. Thus the higher symmetry now has the lower energy. Furthermore, for $\lambda/a \geqslant 1$ the interaction between centered or edge interstitials is attractive for distances larger than five lattice spacings. But for $\lambda/a = 0.25$, the interaction between centered interstitials becomes repulsive for distances $L_x > 5a$. For the edge interstitial, we observe an attractive interaction at distances $L_x < 10a$, and a repulsive interaction at $L_x > 10a$.

As in the previous subsections, we consider here periodicity cells of different sizes, which now contain one vacancy and one interstitial. The vacancy, which we choose as origin, is created in one corner of the periodicity cell and the interstitial is created as close as possible to the center of the cell. Thus, our periodic boundary conditions yield two interlaced superlattices of vacancies and interstitials. For each size of the periodicity cell (L_x, L_y), the closest distance between a

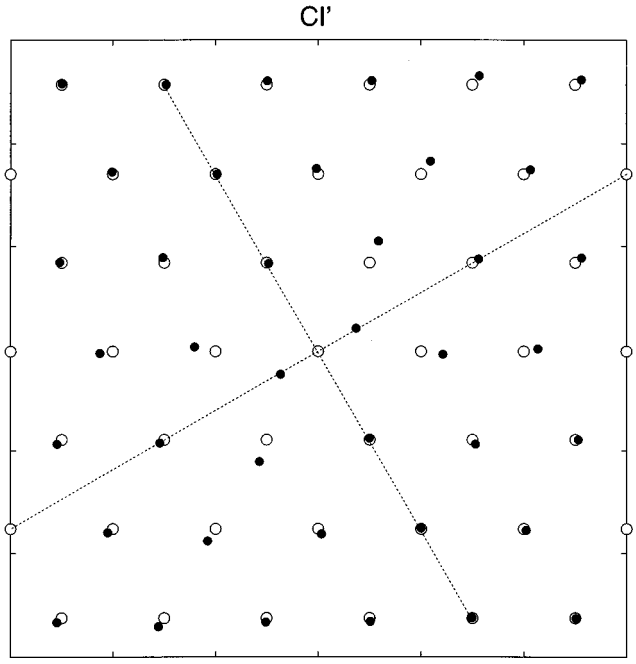

FIG. 6. The new centered interstitial configuration CI′ obtained for the box size $(L_x,L_y)=(5,6\sqrt{3}/2)4a$. Shown is only the central region $6a\times 6a$ of the periodicity cell. The symmetry of the original centered interstitial is threefold, see Fig. 4. Whereas the interaction between interstitials does not change this symmetry, the interaction between a vacancy and an interstitial changes the symmetry of the interstitial, which becomes twofold. This symmetry change occurs in both cases $\lambda/a=100$ and $\lambda/a=0.25$ at $d\leqslant 14.1a$ and $d\leqslant 10.6a$, respectively.

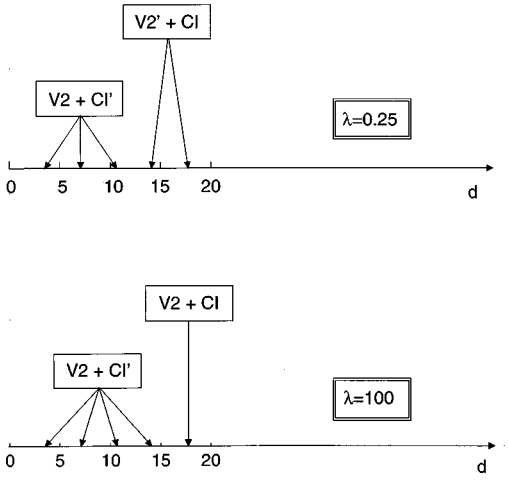

FIG. 7. The various symmetry changes caused by the elastic interaction between a vacancy and an interstitial for $\lambda/a=100$ and $\lambda/a=0.25$. The vacancy is created in one corner of the periodicity cell and the interstitial is created as close as possible to the center of the cell. The plotted axis gives the distance $d\approx L_x/\sqrt{2}$ between the vacancy and the interstitial in units of the lattice spacing. For each value of λ five distances d have been computed ($d/a\approx 17.7,14.1,10.6,7.1,3.5$) corresponding to periodicity cell sizes $(L_x,L_y)=(5,6\sqrt{3}/2)ta$ with $t=5,4,3,2,1$, respectively. The symmetry of the vacancy and interstitial are indicated for each case with the notations defined in the text.

vacancy and an interstitial is then $d\approx L_x/\sqrt{2}$ and the vector connecting them forms an angle $\alpha\approx\pi/4$ with the x direction of our periodicity cell, which coincides with one of the three nearest-neighbor directions of the ideal triangular lattice. Since the number of vortices is not changed by the creation of vacancy-interstitial pairs, the total energy of this superlattice of defect pairs is computed from Eq. (9) [i.e., the correction term in Eq. (17) is zero]. Before we present the energy of the vacancy-interstitial pair, we discuss how the structure of the two point defects changes with their distance.

For $\lambda/a=100$ and infinite distance d between the two defects we expect the configuration with lower energy to consist of a twofold symmetric vacancy V2 and a centered interstitial CI as described in Secs. III B and III C. This is indeed observed for distances $d\approx L_x/\sqrt{2}$ down to $d\approx 17.7a$, i.e., to the periodicity cell size $(L_x,L_y)=(5,6\sqrt{3}/2)5a$. But when d is decreased further, qualitative changes are observed. At $d\approx 14.1a$, i.e., for $(L_x,L_y)=(5,6\sqrt{3}/2)4a$, the vacancy V2 remains unchanged but the symmetry of the interstitial switches from threefold to twofold, see Fig. 6. The center of symmetry now is no longer at the interstitial as it was for the centered and edge interstitials, but at one of the corners of the initial triangle centered at the original interstitial. We denote this new centered interstitial by CI′. The symmetry change of the interstitial may be ascribed to the elastic interaction between these point defects. At smaller distances $d\approx 10.6a$, $d\approx 7.1a$, and $d\approx 3.5a$, i.e., for supercell-sizes $(L_x,L_y)=(5,6\sqrt{3}/2)ta$ with $t=3$, 2, 1, no further deformation is observed, i.e., the relaxed configurations still contain a vacancy V2 and an interstitial CI′.

For $\lambda/a=0.25$ and when the distance between the two defects is infinite, we expect the lower energy configuration to be formed by a twofold symmetric vacancy V2′ and a centered interstitial CI, see Secs. III B and III C. When decreasing the distance between the point defects we again observe the appearance of the twofold symmetric interstitial CI′ shown in Fig. 6, which we observed also for $\lambda/a=100$. But this new interstitial symmetry now appears at smaller distances than in the case of $\lambda/a=100$. This might have been expected, since with $\lambda/a=0.25$ the flux lines interact only with a few neighbor shells, thus the direct magnetic interaction between the point defects becomes of short range and only the indirect elastic interaction matters. For this short λ value we observe this symmetry change of the interstitial for $d\approx 10.6a$. At the same distance d, the vacancy also changes its symmetry, namely, it switches from the V2′ symmetry, observed at large d, to the V2 symmetry commonly observed for $\lambda/a=100$. For isolated vacancies these two symmetries V2′ and V2 have very close energies, see Fig. 2(c). The coexistence between a twofold symmetric vacancy V2 and the twofold symmetric interstitial CI′ is also observed at the smaller distances $d\approx 7.1a$ and $d\approx 3.5a$.

These symmetry changes induced by the elastic interaction between a vacancy and an interstitial are summarized in Fig. 7. The energy of the vacancy-interstitial superlattice is plotted in Fig. 8 versus the cell width L_x for interaction ranges $\lambda/a=100$ and $\lambda/a=0.25$, see also Table II. We expect the total energy of such a superlattice of defect pairs to

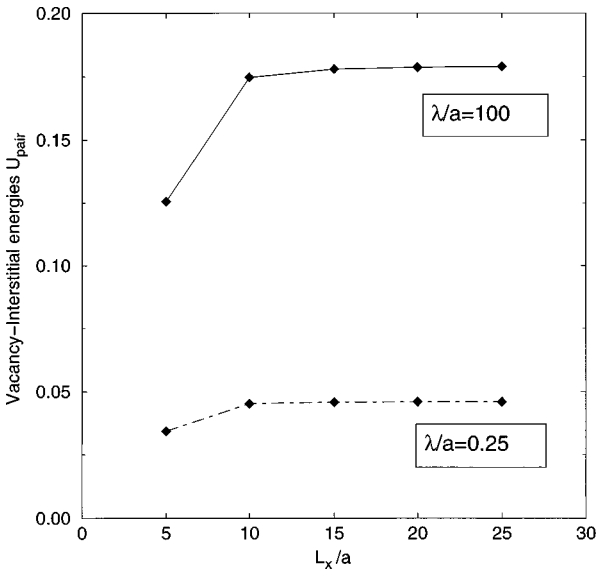

FIG. 8. Supercell size dependence of the energies of the superlattice formed by vacancy-interstitial pairs, for $\lambda/a=100$ (solid line) and $\lambda/a=0.25$ (dash-dotted line). The energies in units of E_0 are plotted versus L_x/a where L_x is one side of the (almost quadratic) periodicity box and a the lattice spacing. The increasing curves in the range $5\leqslant L_x/a\leqslant 25$ show that the interaction between a vacancy and an interstitial is attractive for distances larger than $d\approx L_x/\sqrt{2}\approx 3.5a$ and smaller than $d\approx L_x/\sqrt{2}\approx 17.7a$

exhibit qualitatively the same distance dependence as a single defect pair. From the observed increase of the defect pair energy with increasing cell size $L_x\times L_y$ we thus conclude that *the interaction between a vacancy and an interstitial in the vortex lattice is attractive*. Thus, vacancies attract both other vacancies and interstitials.

IV. SUMMARY AND CONCLUSIONS

In conclusion, we computed the arrangement of vortices around various point defects, and the corresponding defect energies, in an infinite lattice of long parallel Abrikosov vortices in type-II superconductors, using London theory and periodic boundary conditions. In the limit of large London penetration depth λ part of our results should also apply to the short vortices in thin films of thickness $d\ll\lambda$ in perpendicular magnetic field. These films exhibit an effective penetration depth $\Lambda=2\lambda^2/d$ that may become much larger than the vortex spacing a. For distances $r\ll\Lambda$ the interaction between such flat vortices is logarithmic,[23,24] $V(r)\propto\ln(\Lambda/r)$, as the interaction between parallel Abrikosov vortices at short distances $V(r)\propto K_0(r/\lambda)\approx\ln(\lambda/r)$ is for $r\ll\lambda$, cf. Eq. (1). In the case of long-range interaction $\lambda\gg a$, the self-energies of vacancies and interstitials, defined at constant average vortex density B/Φ_0, are very small compared to the binding energy of one vortex, and the interaction between point defects is even smaller.[7,17] Our computations confirm this prediction.

We find that vacancies and interstitials of various symmetries may occur during the relaxation of the vortex lattice. Such a configuration may be called a metastable state if the relaxation procedure remains quasistationary during a large number of iteration steps, but then the relaxation proceeds to a different configuration with lower energy. In particular, we confirm the result of Frey *et al.*[7] that the vacancy configuration with sixfold rotational symmetry, considered in Refs. 5,6, does not have the lowest energy. This vacancy with highest symmetry is metastable, another vacancy with threefold rotational symmetry has somewhat lower energy, and a vacancy with only twofold symmetry has the lowest energy of these vacancy configurations.

In contrast to this, for the interstitials the configuration with higher (threefold) symmetry has lower energy than the interstitial with twofold symmetry. The centered threefold symmetric interstitial has the lowest energy of all point defects, also lower than all vacancy energies. These results apply to the range of interaction lengths $0.25\leqslant\lambda/a\leqslant 100$. A further interesting finding is that the symmetry of an interstitial may change when a vacancy is added even at a large distance of $14.1a$.

For point defect interactions, we find that the interaction between two vacancies is attractive whatever their symmetry is. This contradicts the repulsive interaction between twofold symmetric vacancies found in Ref. 7. We also obtain an attractive interaction between two interstitials for $\lambda/a=1$ and 100. But for $\lambda/a=0.25$, we find that two interstitials repel each other at distances larger than ten lattice spacings.

As can be seen from Figs. 2, 5, and 8, the defect energy U changes only little with increasing distance d between the point defects forming a superlattice. We find that for not too small d in all considered cases these energies approximately follow power laws $U(d)\propto d^{-\alpha}$ with various exponents $1.3\leqslant\alpha\leqslant 4.4$. Note that this implies that the interaction between two isolated point defects of distance r follows the same power law, i.e. $V(r)\propto r^{-\alpha}$. The accuracy of the exponents α obtained by fitting our numerically obtained interaction energies is not very high. Since we were interested mainly in large distances, we exluded the case of smallest cell size from this fitting. Some α values obtained in this way are listed in Table III. One can see that for the interaction between vacancies and edge interstitials the exponent α is approximately 2, but when centered interstitials are involved, exponents between 1.3 and 4.4 are observed in our compu-

TABLE III. The exponents α of power laws $U=A+Bd^{-\alpha}$ which fit the energy of a superlattice of point defects of spacing d by three parameters A, B, and α. The notations for the defect symmetries are given in the text. The exponents α were obtained from the data in Figs. 2, 5, and 8 and in Tables I and II, excluding the case with shortest d. No α is listed in cases when the numerical accuracy did not allow for a fit.

Defect symmetries	$\lambda/a=0.25$	$\lambda/a=1$	$\lambda/a=100$
V6–V6	1.5	2.0	2.1
V3–V3	1.8	2.2	2.4
V2–V2	2.4	2.0	1.8
V2′–V2′	2.3		
EI–EI		2.1	2.1
CI–CI	3.0	1.3	1.5
V2–CI			3.1
V2′–CI	4.4		

tations. This finding indicates that at the considered distances between 10 and 25 flux-line spacings a, and in the considered direction, the exponent α of the observed power-law interaction between point defects is not determined by their symmetry alone, in contrast to what is expected at very large distances in isotropic media.[7]

ACKNOWLEDGMENTS

Stimulating discussions with Uwe Essmann and Roman Mints are acknowledged. This work was supported by the German-Israeli Foundation for Research and Development, Grant No. I-300-101.07/93.

[1] A. A. Abrikosov, Zh. Éksp. Teor. Fiz. **32**, 1442 (1957) [Sov. Phys. JETP **20**, 480 (1965)].
[2] U. Essmann and H. Träuble, Phys. Lett. **24A**, 526 (1967); Phys. Status Solidi **32**, 337 (1968).
[3] H. Träuble and U. Essmann, Phys. Status Solidi **25**, 373 (1968); J. Appl. Phys. **39**, 4052 (1968).
[4] R. Labusch, Phys. Lett. **22**, 9 (1966); E. H. Brandt, Phys. Status Solidi **36**, K167 (1969); Phys. Rev. B **34**, 6514 (1986).
[5] E. H. Brandt, Phys. Status Solidi **35**, 1027 (1969); **36**, 371 (1969).
[6] E. H. Brandt, Phys. Status Solidi **36**, 381 (1969); **36**, 393 (1969).
[7] E. Frey, D R. Nelson, and D. S. Fisher, Phys. Rev. B **49**, 9723 (1994); see also, E. Cockayne and V. Elser, *ibid.* **43**, 623 (1991).
[8] J. R. Clem, Phys. Rev. B **43**, 7837 (1991).
[9] R. Schmucker, Philos. Mag. **35**, 431 (1977); **35**, 453 (1977).
[10] L. Glazman and A. Koshelev, Phys. Rev. B **43**, 2835 (1991).
[11] A. Campbell and J. Evetts, Adv. Phys. **72**, 199 (1972).
[12] R. P. Huebener, *Magnetic Flux Structures in Superconductors* (Springer, Berlin, 1979).
[13] E. H. Brandt and U. Essmann, Phys. Status Solidi B **144**, 13 (1987).
[14] G. Blatter, M. V. Feigel'man, V. B. Geshkenbein, A. I. Larkin, and V. M. Vinokur, Rev. Mod. Phys. **66**, 1125 (1994).
[15] E. H. Brandt, Rep. Prog. Phys. **58**, 1465 (1995).
[16] M. Slutzky, R. G. Mints, and E. H. Brandt, Phys. Rev. B **56**, 453 (1997).
[17] E. H. Brandt, Phys. Rev. B **56**, 9071 (1997).
[18] E. H. Brandt, Phys. Rev. B **34**, 6514 (1986).
[19] A. Yaouanc, P. Dalmas de Réotier, and E. H. Brandt, Phys. Rev. B **55**, 11 107 (1997).
[20] E. H. Brandt, Phys. Rev. Lett. **78**, 2208 (1997).
[21] W. H. Press, B. P. Flannery, S. A. Teukolsky, and W. T. Vetterling, *Numerical Recipes* (Cambridge University Press, Cambridge, 1986).
[22] E. H. Brandt, J. Low Temp. Phys. **53**, 41 (1983); **53**, 71 (1983).
[23] J. Pearl, Appl. Phys. Lett. **5**, 65 (1964).
[24] J. R. Clem, Phys. Rev. B **43**, 7837 (1991).